



# Insight into the electronic and elastic properties of Li-rich- antiperovskite $\text{Li}_3\text{OCl}$ under hydrostatic pressures

F Redjem<sup>1\*</sup>, K Souleh<sup>1</sup>, B Lagoun<sup>2</sup>, H Mebarki<sup>3</sup>, and H Lidjici<sup>3</sup>

1. Laboratoire d'étude et développement des Matériaux Semi-conducteur et Diélectriques (LEDMaScD), Université Amar Telidji, Bp37G 03000 Laghouat, Algerie
2. Laboratoire physique des matériaux (LPM), Université Amar Telidji, Bp37G 03000 Laghouat, Algerie.
3. Laboratoire de matériaux pour Application et Valorisation des Énergies Renouvelables (LMAVER), Université Amar Telidji, Bp37G 03000 Laghouat, Algerie.

E-mail: f.redjem@lagh-univ.dz

(Received 20 April 2024 ; in final form 4 August 2024)

## Abstract

Ab initio calculations were employed to examine the structural, elastic, and electrical properties of  $\text{Li}_3\text{OCl}$ , a cubic antiperovskite compound, under varying pressures. The calculations were performed using first principles density functional theory based on the full potential linearized augmented plane wave (FP-LAPW) method as implemented in a Wien2k package. The Perdew-Burke-Ernzerhof Generalized Gradient Approximation (PBE-GGA) was used as an exchange and correlation potential to investigate equilibrium structural parameters, energy band structure, density of states, and elastic characteristics for the  $\text{Li}_3\text{OCl}$  compound. We computed the Young modulus, Poisson ratio, and elastic anisotropy factor for this compound using elastic parameters. It is concluded that the material is mechanically stable according to the Born stability criteria and behaves in a brittle manner, referring to Pugh's index. Our results show that the predicted structural parameter values at 0 GPa are consistent with previous studies. Additionally, it has been found that the material exhibits a transition phase under a pressure of 1 GPa.

**Keywords:** antiperovskite, elastic properties, electronic structure, ab initio calculations, lithium battery

## 1. Introduction

The antiperovskite materials were first discovered in 1915 and then proposed as energy storage materials [1, 2]. They have crystal structure that is the inverse of the well-known perovskite structure. The chemical formula can be written as  $\text{ABX}_3$ , where A and B are cation and X is anion [1].

Antiperovskites have the same space group and crystal system as conventional perovskites (i.e.,  $\text{Pm}\bar{3}\text{m}$  and cubic) but with inverted cation-anion sites [3]. Their interesting physical properties including superconductivity, high ionic conductivity, good safety features, low activation energy, wide electrochemical window, environmental friendliness, high-energy density and low cost [4–6], make them promising candidates for use in solid-state lithium battery.

Due to its important in energy storage devices [6, 7], a considerable number of studies have been done on Li-rich-Antiperovskite material. On an experimental level,  $\text{Li}_3\text{OCl}$  was synthesized for the first time by Yusheng Zhao et al [6]. They heated molten LiX and LiOH as the starting materials under vacuum for several days:  $\text{LiCl} + 2\text{LiOH} = \text{Li}_3\text{OCl} + \text{H}_2\text{O}$  [3]

On a theoretical level, [9, 10], found that the synthesized material exhibit thermodynamic meta-stability and excellent electrochemical stability against lithium metal, which suggests excellent electrochemical performance. Ziheng Lu et al. [11] investigated the defect chemistry and lithium ion migration in  $\text{Li}_3\text{OCl}$  [11]. They proposed a model for Li-vacancy diffusion, suggesting that Li-vacancies serve as the primary mobile charge carriers. However, the calculated migration energy barrier for a Li-vacancy (~0.3 eV) exceeded the experimentally observed value (0.26 eV) [6]. In addition Chen M-H et al. [12] investigated the presence of dynamical instability in this material. The ionic conductivity was reported by [3, 13]. The mechanical properties calculated by Wu.M et al. [14] suggest that this material is brittle ( $B/G < 1.75$ ). Furthermore, the elastic properties of  $\text{Li}_3\text{OCl}$  have been studied by Zhi Deng et al. [15].

Based on previous literary studies,  $\text{Li}_3\text{OCl}$  has received considerable attention in recent years, leading to significant discoveries to its physical properties. However, there still remain unexplored aspects,

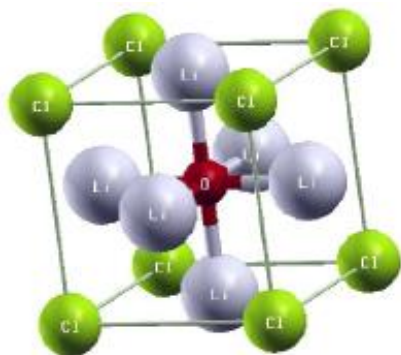


**Figure 1.** The unit cell of the  $\text{Li}_3\text{OCl}$ .

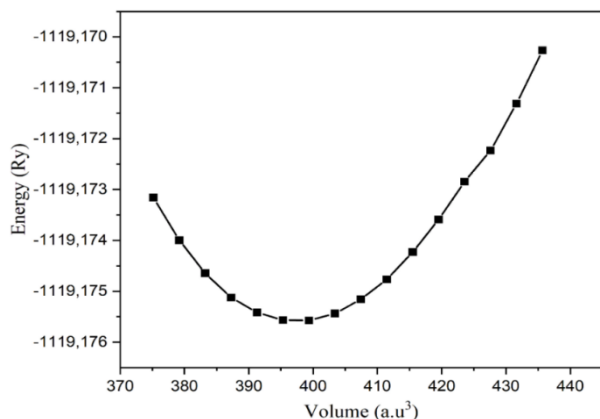


**Figure 2.** Variation of total energy as a function of the unit cell volume for  $\text{Li}_3\text{OCl}$ .

**Table 1.** Computed lattice parameters  $a_0$  ( $\text{\AA}$ ), bulk modulus  $B$  (GPa), pressure derivatives of bulk modulus  $B'$ , equilibrium volume  $V_0$  ( $\text{\AA}$ )<sup>3</sup>, total energy  $E_{tot}$  (Ry), for  $\text{Li}_3\text{OCl}$ .

	$a_0$	$B$	$B'$	$V_0$	$E_{tot}$
This work	3.89	53.15	5.074	59.7	-1119.17
Exp [6]	3.91		-	-	-
Calc [9]	3.8496				
Calc [14]		51.36			
Calc [15]		55.70			

including the effects of pressure on the electronics and elastic properties.

In this study, we have employed first-principles density functional theory (DFT) calculations to investigate the effects of pressure on the electronic and elastic properties of  $\text{Li}_3\text{OCl}$ .

The remainder of this paper is organized as follows: Section 2 will describe the computational methods. The important results of our findings are separately presented in section Results and Discussion for each property of that system, followed by a conclusion.

## 2. Methods

To achieve our goal, all the computations done in this work were performed with the ab-initio calculations using the Wien2k Code [16]. Under various hydrostatic pressures [17], the Perdew-Burke-Ernzerhof (PBE)-GGA approximation were used as an exchange and correlation potential [18]. The plane wave cut-off is taken to be

$R_{\text{MT}}K_{\text{max}} = 7$  where  $R_{\text{MT}}$  the smallest muffin-tin radius and  $K_{\text{max}}$  is the cut-off of the plane waves. For different hydrostatic pressure the reduction of the muffin-tin radius was set to 5%. We set  $L_{\text{max}} = 10$  which is the maximum value of wave function expansion inside spheres. The cut-off energy was selected  $-6.0$  Ry. The k integration over the Brillouin zone is performed using the Monkhorst and Pack scheme [19], where a grid of  $16 \times 16 \times 16$  k-point mesh is chosen. The convergence energy is taken  $10^{-4}$  Ry.

## 3. Results and discussion

### 3.1. Structural properties

Many experimental and theoretical study [6, 9] confirmed that Li-rich antiperovskites  $\text{Li}_3\text{OCl}$  compound is crystallize in  $Pm\bar{3}m$  structure (#221) with the Wyckoff positions of the atoms which are O(0.5 0.5 0.5), Cl (0 0 0) and Li (0.5 0.5 0) as shown in figure 1.

To determine the ground state properties lattice parameter  $a_0$ , volume  $V_0$ , bulk modulus  $B$  and its pressure derivatives  $B'$ , the total energy were calculated for various volumes around the experimental cell volume [6], then the total energy versus the volume are fitted to the empirical Murnaghan's equation of state (figure 2).

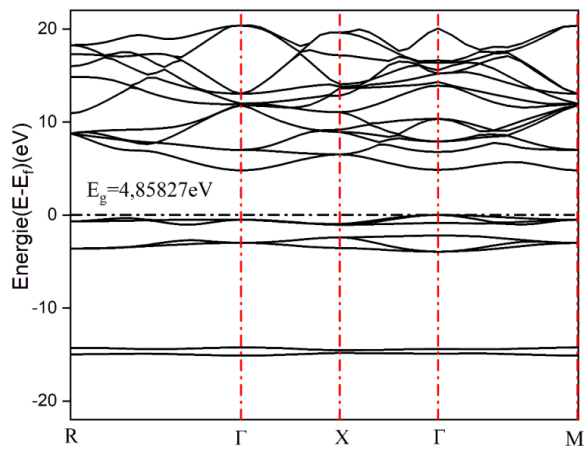
The Obtained results of the  $\text{Li}_3\text{OCl}$  compound and their comparisons values are represented in table 1. We observe that the computed value of lattice parameter is in good agreement with the previous studies [7, 12, 13, 17] were the deviation was about 0.5% and slightly higher than the theoretical value [9]. On the other hand, the computed bulk modulus is in good agreement with previous studies [14, 15].

### 3.2. Electronic properties

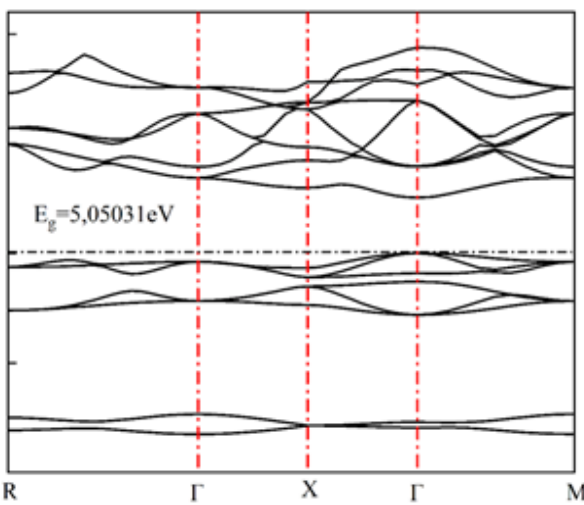
To understand material's electronic behavior, it is essential to determine its band structure and density of states (DOS). These factors provides an insight into how electrons behave within the material. The computed band structure of the antiperovskite at zero pressure, along high symmetry directions in the Brillouin zone, is shown in figure 3a. We observe that the valence band maximum (VBM) occurs at the  $\Gamma$  point, and the conduction band minimum (CBM) also occurs at the  $\Gamma$  point, indicating that this compound possesses a direct band gap. The value of the gap of  $\text{Li}_3\text{OCl}$  material is around 4.85 eV. This significant energy gap makes the compound highly electrochemically stable [9], which is the main characteristic needed for compounds used in energy storage applications [9]. The obtained result of the energy gap is consistent with other calculations [9, 20].

To comprehend more fully the electronic behavior of  $\text{Li}_3\text{OCl}$  we have also calculated the total and the partial Density of state (DOS).

It can be seen that the valence bands are localized in two regions. The lowest state is mainly attributed to Cl-2P states, while the next states below the Fermi level exhibit a hybridized character of O-1S states, with a lesser contribution from Li-1S states. On the other hand, the conduction band is dominated by Cl-3d states, with lesser contributions from Li-2p and O-3p states.



a



b

**Figure 3.** Electronic band structure for  $\text{Li}_3\text{OCl}$  at (a)  $P=0\text{GPa}$  and (b) at  $P=1\text{GPa}$ .

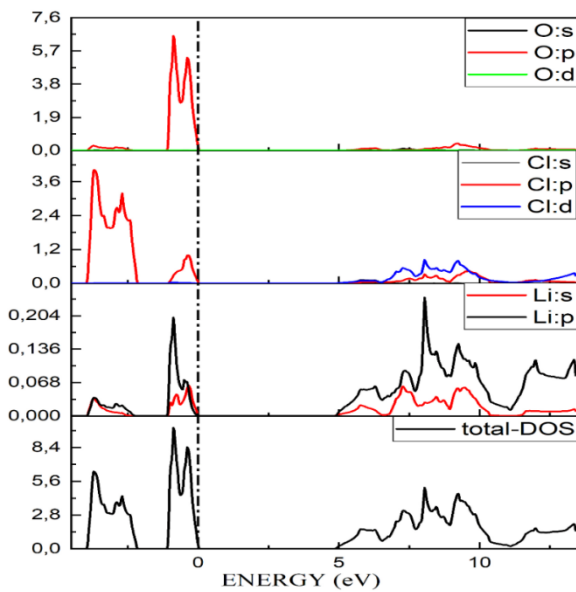


**Figure 4.** Calculated density of states of  $\text{Li}_3\text{OCl}$  at  $P=0\text{GPa}$ .

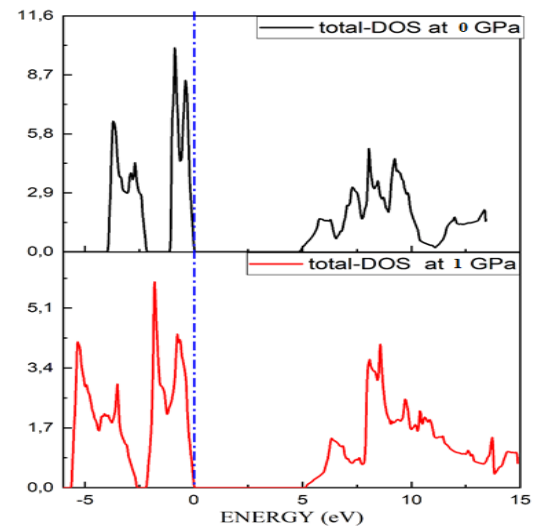


**Figure 5.** Calculated total density of states at  $P=0\text{GPa}$  and  $P=1\text{GPa}$ .

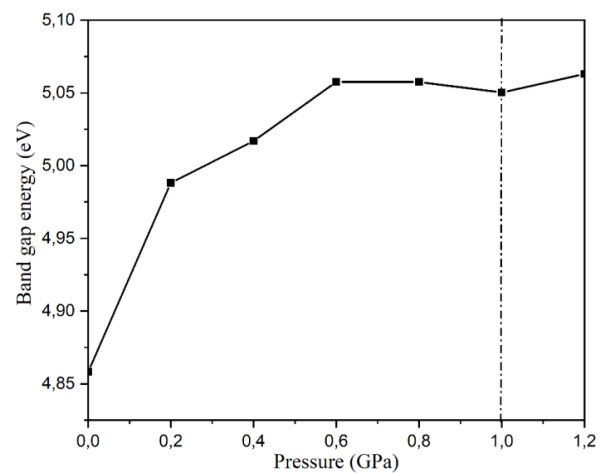


**Figure 6:** Variation of the gap with applied pressure.

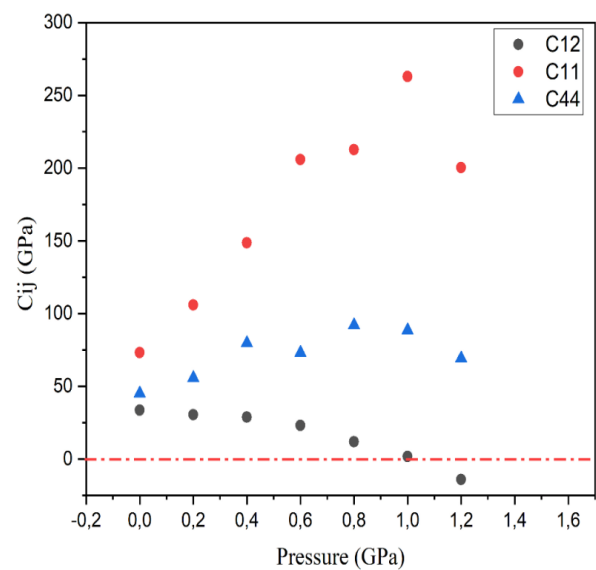


**Figure 7.** The pressure dependence of the three computed elastic constants,  $C_{ij}$ .

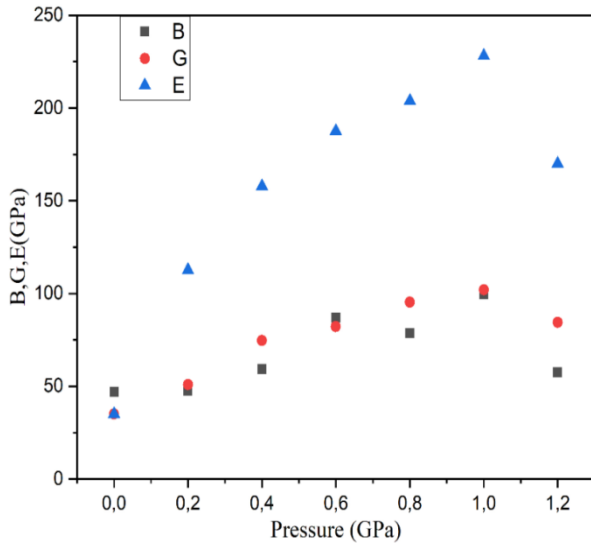


**Figure 8.** . The pressure dependence of B, G, and E.

**Table 2.** Elastic constants  $C_{ij}$  (GPa) , shear modulus G (GPa), Young Modulus E (GPa), Poisson's ratio ( $\nu$ ), Anisotropy factor (A) of  $\text{Li}_3\text{OCl}$  under zero pressure.

	This work	alc[14]	alc[15]
$C_{11}$	73.2870	93.683	102.90
$C_{12}$	38.312	30.20	32.10
$C_{44}$	45.1894	43.33	46.10
G	32.47	38.25	41.50
E	80.29	91.93	99.70
B/G	1.63	1.35	1.35
$\nu$	0.24	0.20	0.20
A	3.6187	-	-

As the antiperovskite  $\text{Li}_3\text{OCl}$  is a brittle compound [14], the applied hydrostatic pressure ranges from 0 to 1 GPa with increments of 0.2 GPa. The effect of external pressure on the material's electronic properties can be observed by comparing the DOS at 0 GPa to those computed at 1 GPa, as illustrated in figure 5. We observe a discernible alteration in the shape of the valence band as the number of states within this band decreases with increasing pressure.

Furthermore, the drawing illustrating the variation of the gap with applied pressure in figure 6 shows that the gap increases with increasing pressure. Referring to the figure 3a and figure 3b we notice a clear contraction of the conduction band with rising pressure accompanied by a decrease in the energy of the valence band leading to an increase in the energy gap with rising pressure.

### 3.3. Elastic properties

The study of elastic constants holds significant interest due to its (their) fundamental role in understanding the mechanical behavior of materials. These constants quantify a material's response to external forces and deformation, providing crucial insights into its elasticity, stiffness, and resilience.

The cubic structure of  $\text{Li}_3\text{OCl}$ , belonging to the subgroup  $\text{Pm}\bar{3}\text{m}$  [6] , requires the determination of three elastic constants ( $C_{11}$ ,  $C_{12}$ , and  $C_{44}$ ) to characterize its mechanical

properties. The calculated elastic constants are presented in table 2. Notably, our obtained constants for  $C_{11}$ ,  $C_{12}$ , and  $C_{44}$  are slightly higher compared to references [14] and [15], with the exception of  $C_{11}$ .

To ensure the mechanical stability of a lattice under zero-pressure conditions, it is essential to satisfy the Born stability criteria [21] , which are defined as follows:  $C_{11}-C_{12}>0$ ,  $C_{11}>0$ ,  $C_{44}>0$ , and  $C_{11}+2C_{12}>0$  . Our computed elastic constants meet these criteria, confirming the material's stability at zero pressure.

The pressure dependence of the three computed elastic constants,  $C_{ij}$ , is illustrated in Figure 7. It is clear that both  $C_{11}$  and  $C_{44}$  increase with rising pressure until reaching an applied pressure of 1 GPa, after which they begin to decrease. On the other hand, the elastic constant  $C_{12}$  exhibits a decreasing trend as pressure increases, crossing the 0 GPa mark at 1.0 GPa.

Building upon the previous discussion, our material  $\text{Li}_3\text{OCl}$  can withstand hydrostatic pressure up to a certain threshold, typically around 1GPa. Beyond this point, it undergoes a phase transition [22].

Table 2 also includes other calculated mechanical properties of the  $\text{Li}_3\text{OCl}$  material. These properties, derived from the three elastic constants ( $C_{ij}$ ), confirm the significance of accurately calculating elastic constants. For a solid, bulk modulus (B) , shear modulus(G)and Young's modulus (E) among The most important elastic parameters of materials. Bulk modulus (B) indicates the resistant of compressibility against hydrostatic pressure and shear modulus represents a material's resistance to deformation by shear stress [23] . Young's modulus is used to measure the stiffness of the materials [24] . Using Voigt (V), Reuss (R), and Hill (H) approximations [25], the bulk modulus (B) ,shear modulus (G) and young's modulus (E) are determined for cubic  $\text{Li}_3\text{OCl}$ , as follows [26]

$$B_V = B_R = B = \frac{C_{11}+2C_{12}}{3} , \quad (1)$$

$$G = \frac{1}{2} (G_V + G_R) , \quad (2)$$

$$E = \frac{9BG}{(3B+G)} , \quad (3)$$

Referring to the values in table 2, we can see that these three parameters are low, indicating that the material is soft [24] . To verify whether the material behaves in a ductile or brittle manner, Pugh formulated a simple relation between bulk modulus and shear modulus (B/G) [27]. If this ratio is less than 1.75, it means the material behaves in a brittle manner; otherwise, it is ductile. In our case, the ratio is 1.63, indicating that the material is brittle, consistent with other theoretical calculations [14] .

The pressure dependence of B, G, and E are displayed in figure 8 . We observe the three parameters are increase with rising pressure until reaching an applied pressure of 1 GPa, after which they begin to decrease with increasing pressure indicating that the material cannot resist more than 1 GPa hydrostaique pressure.

The Poisson's ratio ( $\nu$ ) provides insight into the type of bonding present in a material. It's Calculated based on bulk modulus and shear modulus as follows [28]

$$\nu = \frac{(3B-2G)}{2(3B+G)} , \quad (4)$$

The Poisson's ratio ( $\nu$ ) ranging between -1 and 0.5. Ionic bonding predominates when  $\nu$  falls between 0.1 and 0.33, while metallic bonding dominates for  $\nu$  greater than 0.33 [23]. Referring to the table 2 the Poisson's ratio is 0.24 means the ionic bonding predominates. In ionic crystals, interatomic forces are non-central when  $\nu$  is between 0.1 and 0.25, indicating that our material exhibits non-central interatomic forces.

The elastic anisotropy parameter,  $A$ , offer valuable insights into the principal axes of stiffness within a material. It's given by [23]

$$A = \frac{2C_{44}}{(C_{11}-C_{12})}, \quad (5)$$

Elastic anisotropy parameter value less than 1 indicates that the material's stiffest axes align with the (100) cube orientation, whereas a value greater than 1 suggests stiffness along the (111) body diagonal [29]. Consulting the table 2, the value computed shows clearly that  $\text{Li}_3\text{OCl}$  material exhibits anisotropic features.

#### 4. Conclusion

In this work, we studied the structural, electrical, and

elastic characteristics of  $\text{Li}_3\text{OCl}$  using first principles density functional theory based on the full potential linearized augmented plane wave (FP-LAPW) method implemented in a Wien2k package with the PBE-GGA exchange and correlation potentials. The volume optimization approach was used to optimize lattice constants, which produced findings that are consistent with experimental evidence and earlier theoretical work. DOS and electronic band plots revealed the insulating nature of the compound. As the compound is brittle and can resist just 1 GPa before its transformation phase, so there is no much effect on the band structure and DOS except for an increasing energy gap under rising pressure prior to the phase transition. The elastic features are computed using IRelast package. The obtained results are very close to previous studies. The material is mechanically stable at zero pressure and show a brittle features according to Pugh's index. The type of bonding is found ionic with interatomic non central forces.

#### References

1. Z Deng, et al, *InfoMat* **4** (2022) e12252.
2. P Hartwig, A. Rabenau, and W. Weppner, *J. Less-Common Met.* **78** (1981), 227.
3. J Zheng et al , *ACS Mater.* **1** (2021) 92.
4. E Quartarone and P. Mustarelli, *Chem. Soc. Rev.* **40** (2011) 2525.
5. Y Wang, et al., *Nat. Mater.* **14** (2015) 1026.
6. Y Zhao et al Chem soc, **134** (2012) 15042.
7. M Wu, et al., *Appl. Surf. Sci.* **510** (2020)145394.
8. V Thangadurai and W Weppner, *Ionics* **12** (2006) 81.
9. Y Zhang et al , *Phys Rev B*, **87** (2013) 134303.
10. X Lü, et al., *Adv. Sci.* **3** (2016) 1500359.
11. Z Lu et al , *Phys. Chem. Chem. Phys.* **17** (2015) 32547.
12. M H Chen, A Emly, and A Van der Ven, *Phys. Rev. B*, **91** (2015) 214306.
13. M H Braga, et al., *J. Mater. Chem. A*, **2** (2014) 5470.
14. M Wu, et al., *J. Mater. Chem. A*, **6** (2018) 1150.
15. Z Deng , *J. Electrochem. Soc* **163** (2016) A67.
16. K Schwarz and P Blaha, *Comput. Mater. Sci* **28** (2003) 259.
17. M Jamal, et al., *J. Alloys Compd.*, 735 (2018) 569.
18. J P Perdew, K Burke, and M Ernzerhof, *Phys. Rev. Lett.* **77** (1996) 3865.
19. J Hendrik et al, *Phys. Rev. B.* **13** (1976) 5188.
20. W Xuelong et al , *Energy Storage Sci. Technol.* **5** (2016) 725.
21. M Born Math. Proc. Camb. Philos. Soc, **36** (1940) 160.
22. Gomis, et al., *J. Appl. Phys*, **116** (2014) 133521.
23. S Ayhan and G Kavak, *Mater. Res. Express*, **6** (2019) 0865e9.
24. Y O Ciftci, M Evecen, and İ O Alp, *J. Mol. Model.* **27** (2021) 1.
25. E W Kammer and J V Atanasoff, *Phys. Rev.* **62** (1942) 395.
26. R Paudel and Z Jingchuan, *J. Supercond Nov. Magn.* **31** (2018) 1.
27. S F Pugh, *London Edinburgh Philos. Mag. J. Sci.* **45** (1954) 823.
28. F Tran , *Phys Rev B*, **75** (2007) 11513.
29. C M I Okoye, *Comput. Mater. Sci.* **92** (2014) 141.